AGU PUBLICATIONS

Journal of Geophysical Research: Atmospheres

Supporting Information for

Intercomparison of atmospheric Carbonyl Sulfide (TransCom-COS; Part one): Evaluating the impact of transport and emissions on tropospheric variability using ground-based and aircraft data

Marine Remaud[1], Jin Ma[2], Maarten Krol[2,3], Camille Abadie[1], Mike Cartwright[4,5], Prabir Patra[6], Yosuke Niwa[7,8], Christian Rodenbeck[9], Sauveur Belviso[1], Linda Kooijmans[3], Sinikka Lennartz[10], Fabienne Maignan[1], Martyn P. Chipperfield[11,12], Richard J. Pope[11,12], Jeremy J. Harrison[11,12], Christopher Wilson[11,12] and Philippe Peylin[1]

[1] Laboratoire des Sciences du Climat et de l'Environnement, CEA-CNRS-UVSQ, UMR 8212, IPSL, Gif-sur-Yvette, France

[2] Institute for Marine and Atmospheric Research, Utrecht University, Utrecht, the Netherlands

[3]Meteorology and Air Quality, Wageningen University and Research, Wageningen, the Netherlands

[4]School of Physics and Astronomy, Space Park Leicester, University of Leicester, Leicester, UK

[5]National Centre for Earth Observation, Space Park Leicester, University of Leicester, Leicester, UK

[6]Research Institute for Global Change, JAMSTEC, Yokohama 236-0001, Japan

[7]National Institute for Environmental Studies, 16-2 Onogawa, Tsukuba, Ibaraki, 305-8506, Japan

[8]Meteorological Research Institute, 1-1 Nagamine, Tsukuba, Ibaraki, 305-0052, Japan

[9]Max Planck Institute for Biogeochemistry, Jena, Germany

[10]Institute and Chemistry and Biology of the Marine Environment, University of Oldenburg, Oldenburg, Germany

[11]School of Earth and Environment, University of Leeds, Leeds, UK

[12]National Centre for Earth Observation, University of Leeds, Leeds, UK

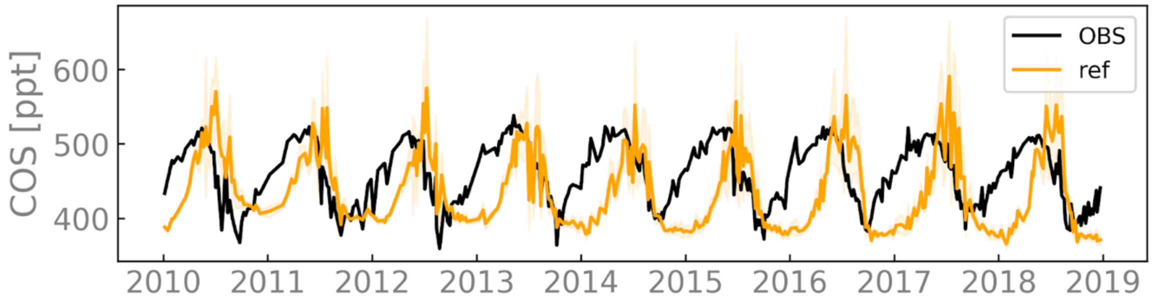

Figure S1. Temporal evolution of the surface COS mixing ratio at site BRW as observed (black) and simulated by several Atmospheric Transport Models (orange) using the **Ctl** scenario. The full line in orange is the averaged concentrations simulated by all transport models and the shaded area is the standard deviation at each time step of the simulated concentrations by all transport models.The simulated COS abundances have been shifted of 396 ppt, which is the observed concentrations averaged over all surface sites for January 2010.

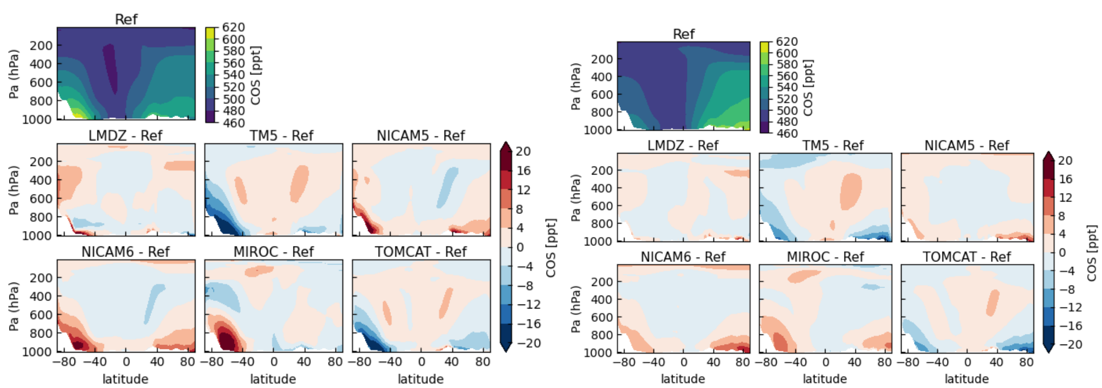

Figure S2: Zonal mean mole fraction of COS in ppt for the reference for the **Ctl** scenario (top row). The reference is the average of COS over all transport models. Second and third rows: Zonal mean mole fraction difference between each transport model and the reference. Left: The zonal mean is averaged in winter (DJF) from 2012 to 2018. Right: The zonal mean is calculated from 2012 to 2018 (annual mean).

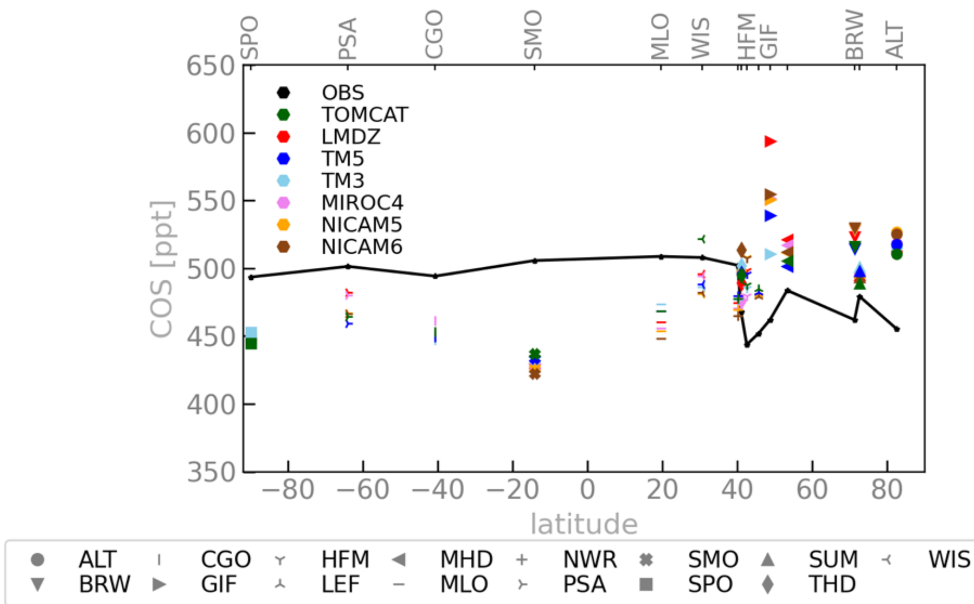

Figure S3: Comparison of the latitudinal variations of the COS abundance simulated by several transport models using the **Ctl** surface flux dataset (colored dots) with the observations (black line) averaged over the years 2012-2019. The simulated COS abundances have been shifted such that the means are the same as the mean of the observations (~500 ppt). The curves have been detrended and filtered to remove the synoptic variability. The value at site GIF simulated by the TOMCAT ATM was removed as it was an outlier (value above 755 ppt).

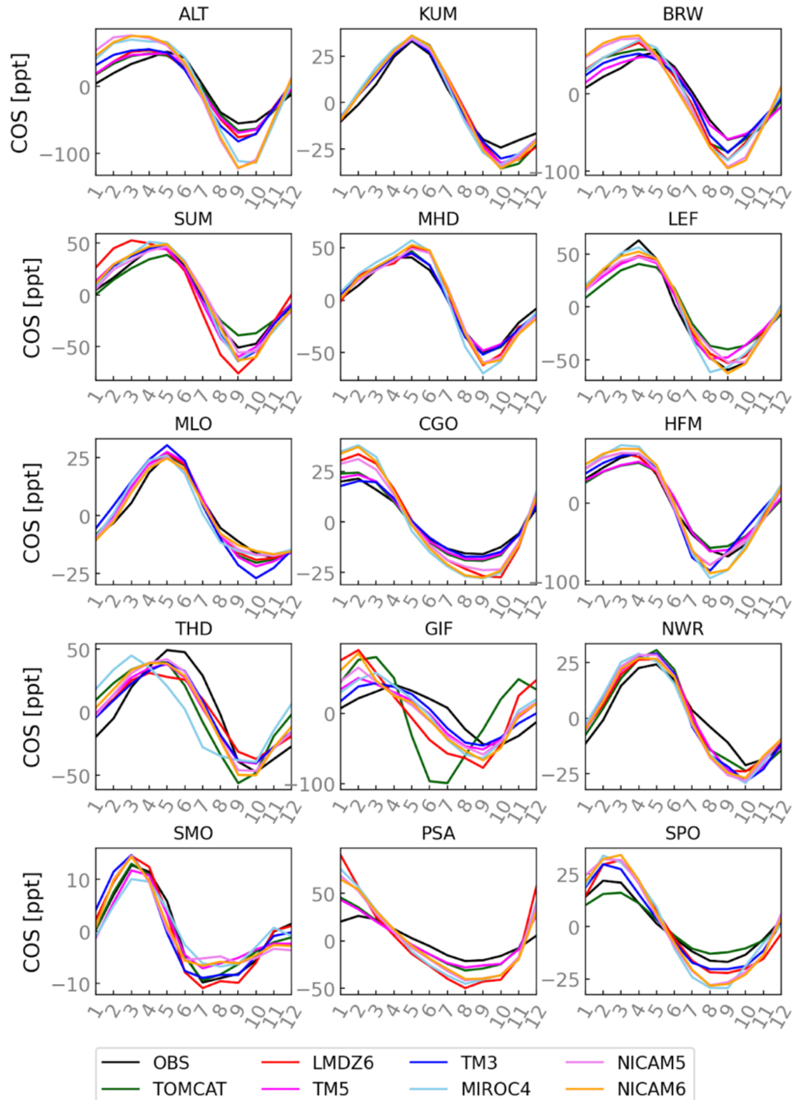

Figure S4 : Mean seasonal cycle of the observed (black) and simulated (color) COS mixing ratios at 15 surface sites for the **Ctl** scenario. The curves have been detrended and filtered to remove the synoptic variability.

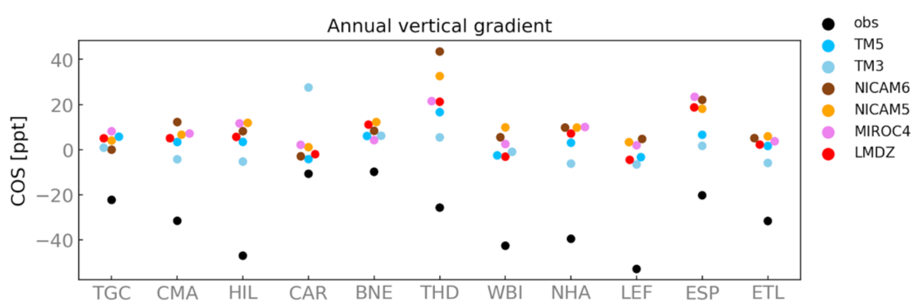

Figure S5. Annual mean observed and simulated COS gradient between 1 and 4 km at each airborne station for the Ctl scenario. For each subregion, the monthly COS gradients are calculated by averaging the differences in COS concentrations between 1 and 4 km over all the vertical profiles.

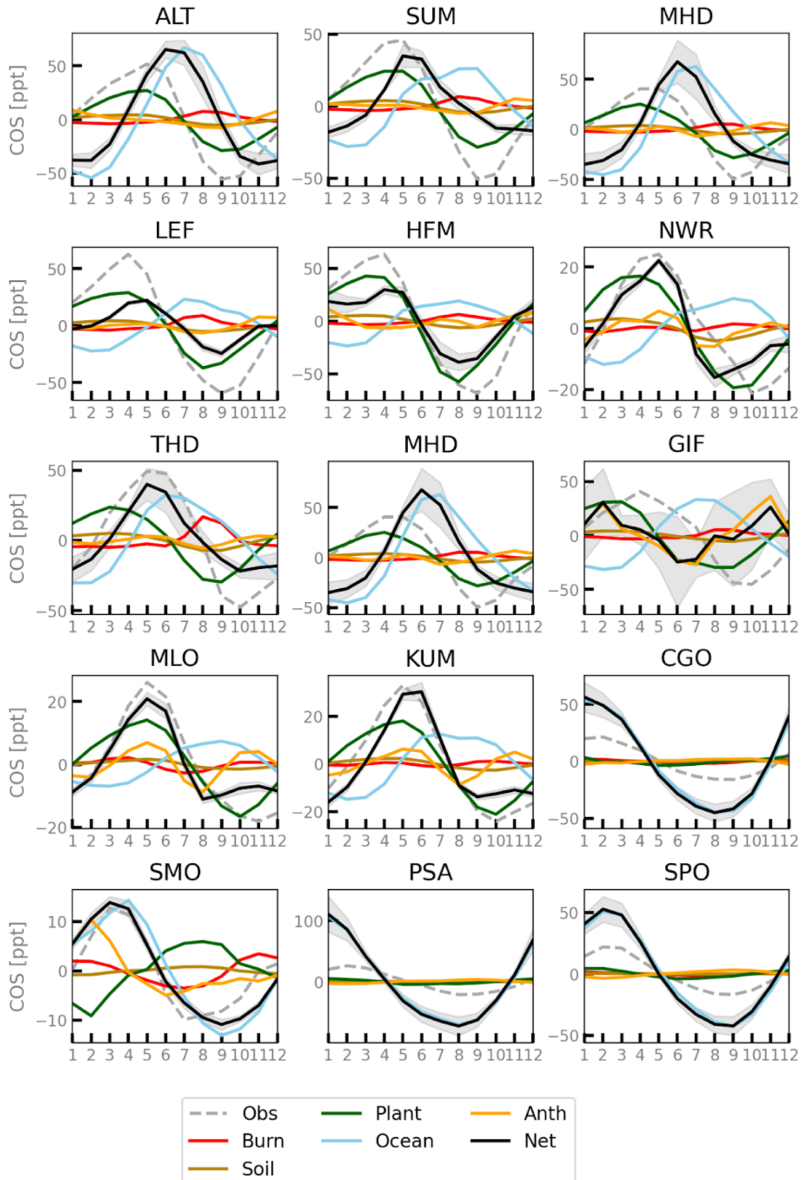

Figure S6: Simulations of the seasonal cycle of tropospheric COS mixing ratios at several surface stations averaged over all transport models. The shaded area is the standard deviation around the mean COS seasonal cycle associated with the different transport models. The dotted black line represents the observed seasonal cycle.

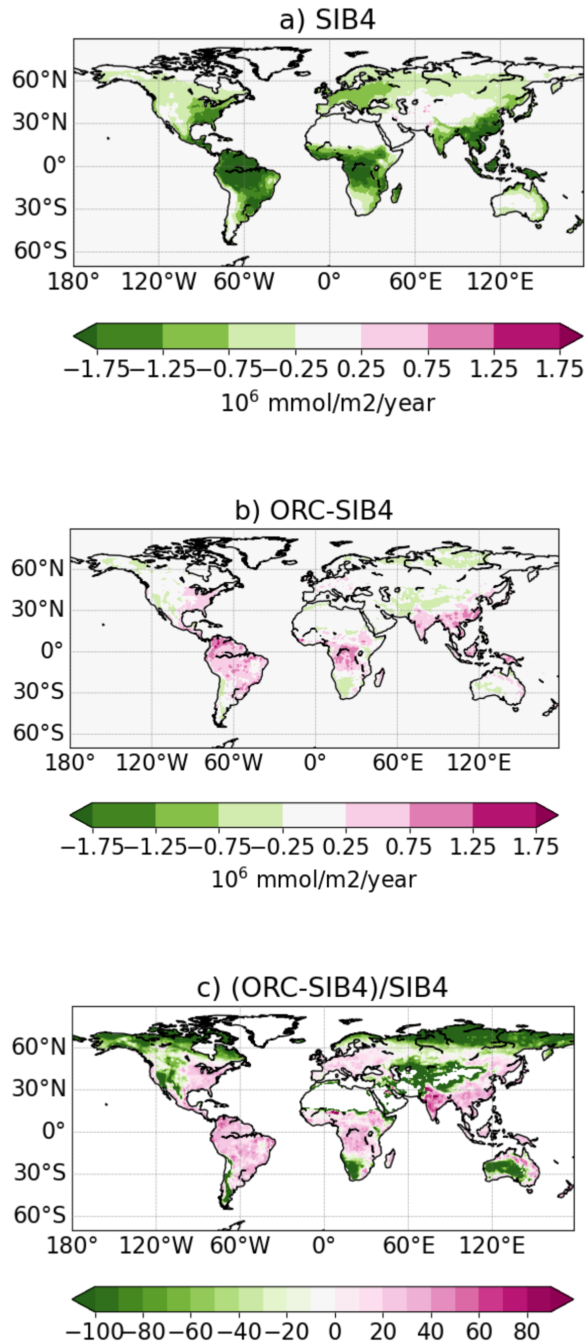

Figure S7: a) Climatology of the biosphere flux of COS (mmol/m^2/yr) in the SIB 4 LSM, b) Climatology of the difference of the biosphere flux (mmol/m^2/yr) between the ORCHIDEE LSM and the SIB 4 LSM. c) Same as b) but in terms of percentage.

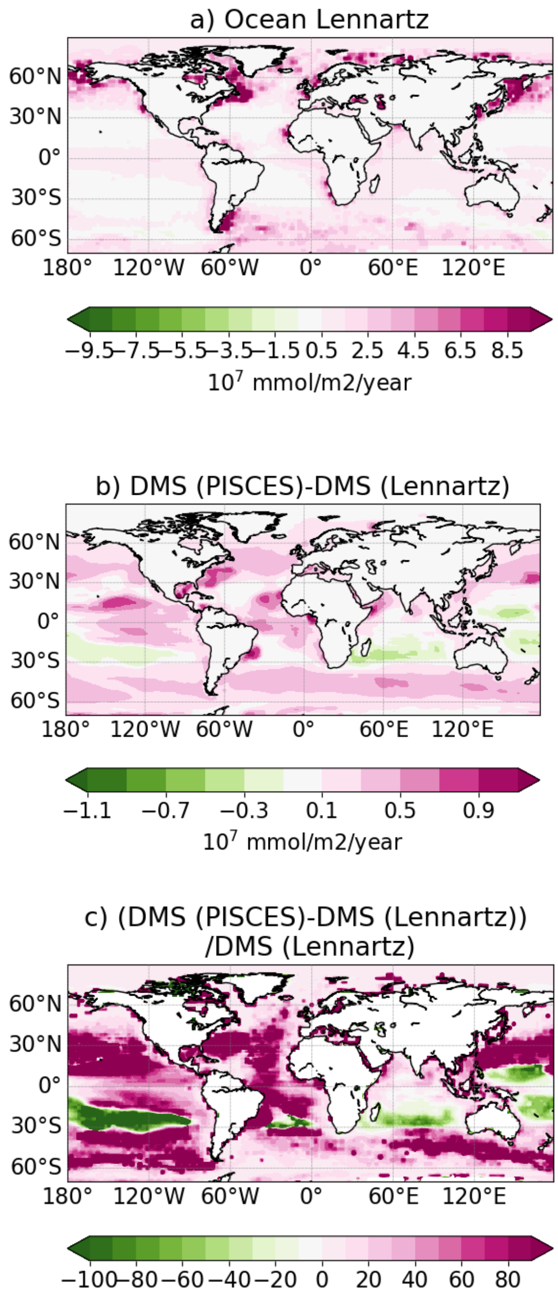

Figure S8 a) Climatology of the ocean flux (mmol/m^2/yr) using the Lennartz et al., 2017 DMS fluxes, b) Climatology of the difference of the ocean flux (mmol/m^2/yr) between the DMS fluxes of Lennartz et al., 2017 and the DMS fluxes simulated by the NEMO-PICSES Ocean Model. c) Same as b) but in terms of percentage.

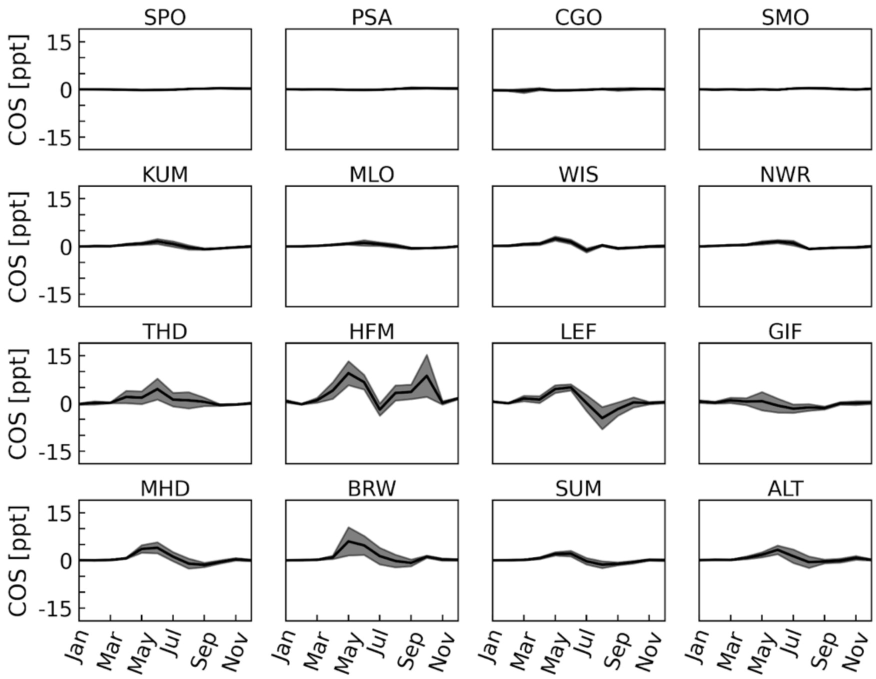

Figure S9 Difference of monthly mean COS mole fractions between the **Diurnal** scenario and the **Ctr** scenario (without the soil fluxes) at each surface station for the year 2015. At each site, the solid line is the mean COS mole fraction across all models, and the shaded envelope represents the standard deviation around the mean. Here, only the vegetation fluxes contribute to the difference of COS mole fractions.

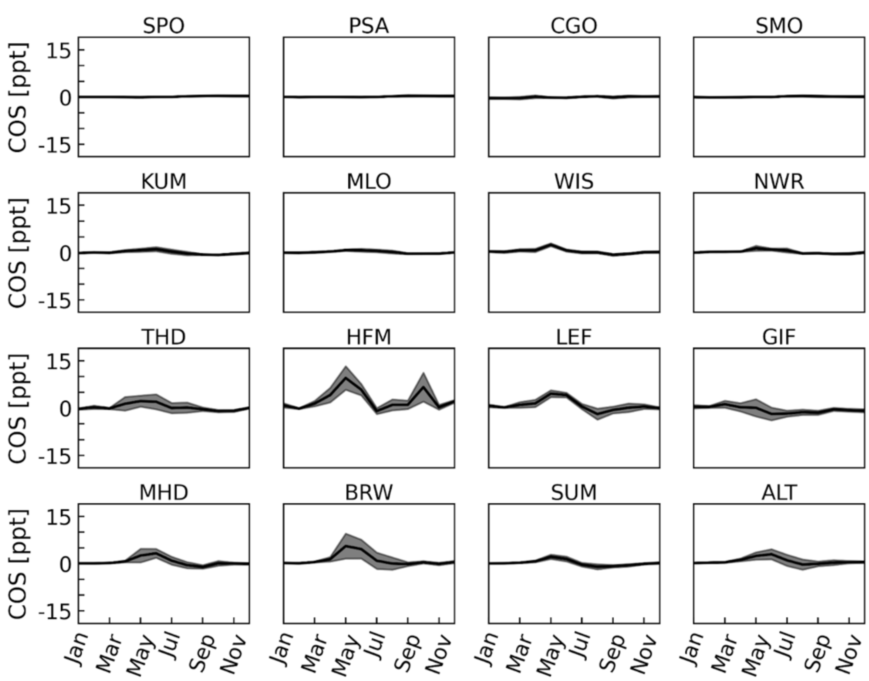

Figure S10 Difference of monthly mean COS mole fractions between the **Diurnal 2** scenario and the **Bio 2** scenario at each surface station for the year 2015 with the LSM

ORCHIDEE. At each site, the solid line is the mean COS mole fraction across all models, and the shaded envelope represents the standard deviation around the mean.

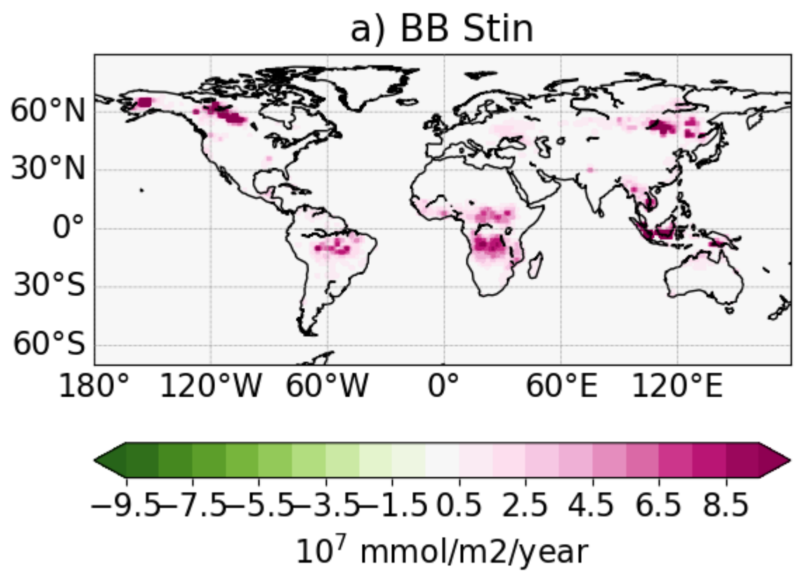

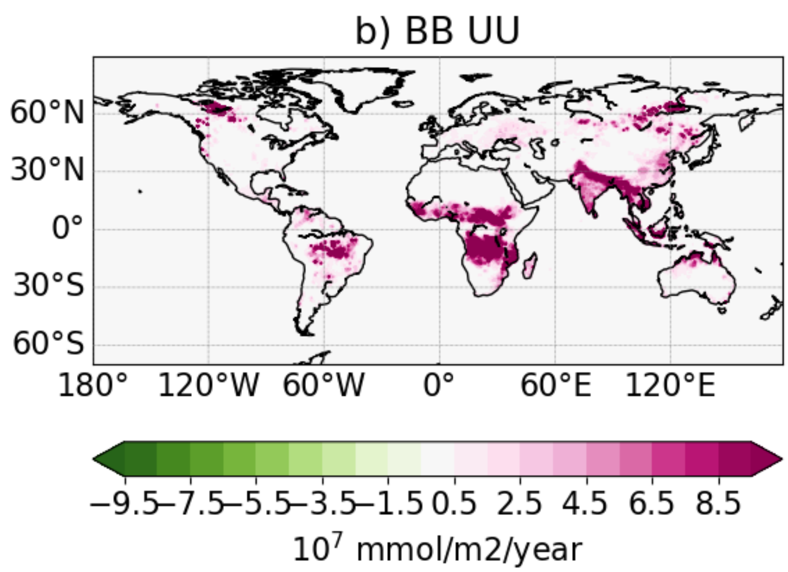

Figure S11: a) Climatology of the biomass burning flux (mmol/m^2/yr) from Stinecipher et al., 2019. b) Climatology of the biomass burning flux (mmol/m^2/yr) from Ma et al., 2021, which takes into account the biofuel use.